Endocrine, *vol. 25, no. 1, 61–67, October 2004* 0969–711X/04/25:61–67/$25.00

Comparison of Metabolic Oscillations from Mouse Pancreatic Beta Cells and Islets

Craig S. Nunemaker and Leslie S. Satin

Department of Pharmacology and Toxicology, School of Medicine, Virginia Commonwealth University Medical Center, Richmond, VA 23298

Rhythmic insulin secretion from pancreatic islets is the culmination of many processes both intrinsic and extrinsic to the beta cell. We wished to examine and compare endogenous metabolic oscillations in islets and isolated single beta cells that underlie secretion. Fluorescence patterns of rhodamine 123, an indicator of mitochondrial membrane potential ($\Delta\Psi_m$), were analyzed for period and amplitude of oscillations using two methods: CLUSTER7 and fast Fourier transform (FFT). The period of $\Delta\Psi_m$ oscillations was greater in islets (271 ± 21 s, $n = 34$) compared to dispersed beta cells (180 ± 10 s, $n = 54$) by FFT analysis ($p < 0.0005$). CLUSTER7 confirmed differences in period and also detected oscillatory amplitude differences between beta cells (12.0 ± 0.8) and islets (7.1 ± 2.3% of baseline fluorescence, $p < 0.0001$). Depolarizing responses to the mitochondrial poison NaN_3 were reduced in beta cells (35 ± 4%) vs islets (58 ± 9%), and hyperpolarizing responses to the calcium channel blocker nifedipine were enhanced in beta cells (15 ± 4%) vs islets (8 ± 1%), suggesting that mitochondria in dispersed beta cells were less energized than those in intact islets ($p < 0.005$), possibly due to elevated intracellular calcium. These findings suggest that individual beta cells possess the proper machinery to generate metabolic oscillations. Differences in oscillatory period, $\Delta\Psi_m$, and nifedipine response suggest that incorporation into islets provides beta cells with additional modulatory influences.

Key Words: Mitochondria; islet; beta-cell; oscillation; rhythm; metabolism; rhodamine.

Introduction

Insulin, a crucial hormone for regulating blood glucose, is secreted from beta cells, which are encapsulated in islets of Langerhans. Several studies provide evidence that beta cells may have all the machinery to produce rhythms in intracellular processes and insulin secretion *(1,2)*, but incorporation into islets may significantly alter the activity of individual beta cells *(3,4)*. Single beta cells, for example, are well known to secrete more insulin when incorporated into islets as evidenced by differences in capacitance measures of exocytosis *(5)* and effects of gap junction expression on secretion *(6,7)*. When directly compared, differences in intracellular calcium ($[Ca^{2+}]_i$) have also been measured between islets and beta cells *(3,4)*.

Patterns of insulin secretion from islets are similar in period (3–10 min) to oscillations in oxygen *(8)*, intracellular calcium *(2–4)*, and glucose *(8,9)*, suggesting that metabolic oscillations may direct or modulate rhythmic insulin secretion. Another marker of cell metabolic activity is mitochondrial membrane potential ($\Delta\Psi_m$). Previous studies using the dye rhodamine 123 (rh123) to measure mitochondrial activity established that $\Delta\Psi_m$ hyperpolarizes in response to increased glucose in beta cells *(10–13)*, consistent with the known action of glucose metabolism to increase the proton gradient that drives mitochondrial ATP production *(14)*. Oscillatory changes in rh123 have been observed previously in both dispersed beta cells *(11)* and islets *(12,13)*, but a direct and systematic comparison between beta cells and islets has been lacking. The primary goal of this study was to examine patterns of rh123 fluorescence oscillations using two mathematical algorithms, fast Fourier transform (FFT) and CLUSTER7 pulse analysis, to ascertain if beta cells and islets differ in their metabolism.

Results

To compare patterns of metabolic activity between dispersed beta cells and islets, we utilized two pulse detection algorithms to analyze patterns of rh123 fluorescence: FFT and CLUSTER7. Each method was first tested on non-rhythmic data series acquired by monitoring fluorescence from rhodamine-coated beads to serve as controls. Signals from beads were stable, as shown by a representative example of rh123 fluorescence plotted vs time in Fig. 1A, and generated the corresponding spectral profile shown in Fig. 1B. In none of the 23 bead clusters tested were any "rhythms" detected by either FFT or CLUSTER7, using the parameters for detection described in the methods.

Received September 8, 2004; Revised September 23, 2004; Accepted September 24, 2004.

Author to whom all correspondence and reprint requests should be addressed: Dr. Leslie S. Satin, Department of Pharmacology and Toxicology, Virginia Commonwealth University, P.O. Box 980524, Richmond, VA 23298. E-mail: lsatin@hsc.vcu.edu

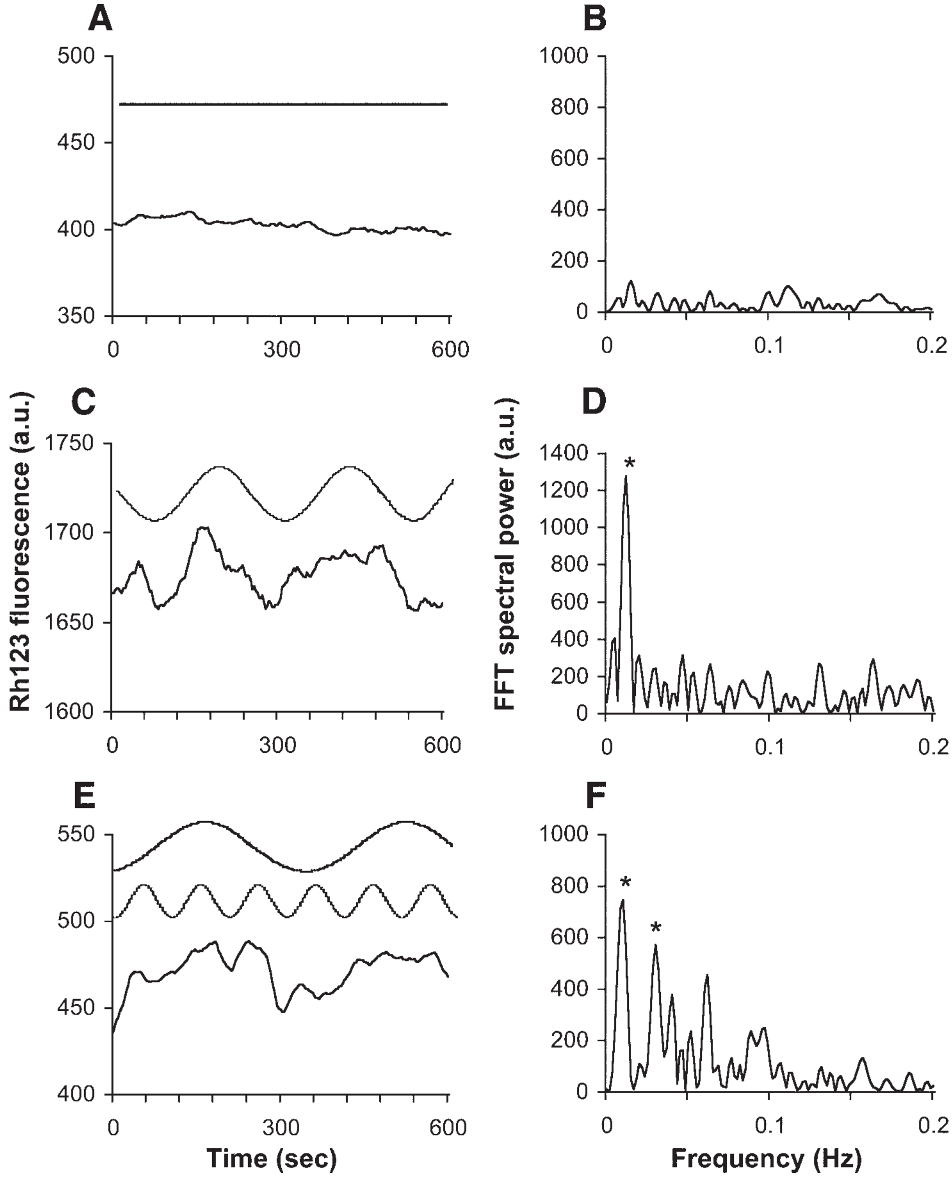

Fig. 1. Analysis by fast Fourier transform (FFT) identifies distinct rhythms. (**A,C,E**) Plot of rh123 fluorescence intensity vs time for a cluster of rhodmaine-coated beads (control, **A**) and two representative islets (**C,E**) during 11.1 m*M* glucose control conditions. Sinusoidal waves sketched above each trace illustrate rhythms identified as significant by the FFT analysis. (**B,D,F**) Power spectra corresponding to traces in **A,C,** and **E**. Asterisks mark significant peaks in spectral output corresponding to rhythms of different frequencies.

Metabolic Oscillations Detected by FFT Analysis Are Faster in Dispersed Beta Cells

We next investigated data acquired from 54 beta cells and 34 islets. Spectral analysis by FFT demonstrated rhythms in 70% of beta cells and 68% of islets. A representative example of rhythmic mitochondrial activity is shown from an islet with its dominant period shown in Fig. 1C, and its corresponding spectral profile shown in Fig. 1D. Rhythms of multiple periodicities were also detected in approx 25% of beta cells and 25% of islets (see example in Figs. 1E,F). Dominant periods in dispersed beta cells were approx 50% faster on average than in islets, while the robustness of rhythms as measured by the magnitude of the dominant spectral power did not differ significantly between groups (see Fig. 3 for summary). These findings confirm that metabolic rhythms are present in dispersed beta cells and suggest that incorporation into an islet is associated with slower rhythms.

The relationship between the size of the beta-cell groups and their period was also investigated. As mentioned, most beta-cell ROIs consisted of individual cells measuring approx 10–12 μm in diameter; however, some groups of cells were used as ROIs with diameters up to 30 μm. The mean period of cells with diameters 10–12 μm, 173 ± 13 s ($n = 22$) as calculated by FFT, did not differ significantly from cell groups, which were >20 μm in diameter (142 ± 21, $n = 5$, $p > 0.24$).

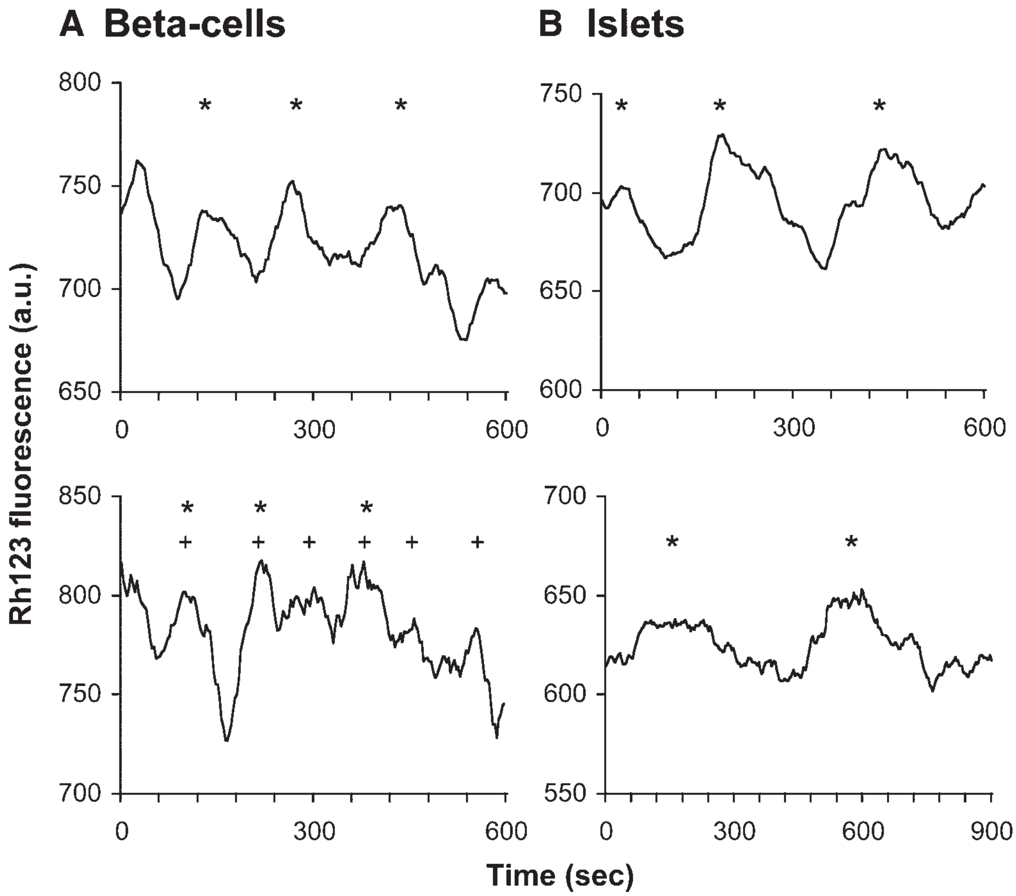

Fig. 2. Analysis by CLUSTER7 confirms findings by FFT. Two representative examples of patterns of rh123 fluorescence from single beta cells (**A**) and islets (**B**). Data are plotted as rh123 fluorescence vs time. Asterisks indicate peaks of increased fluorescence using a minimum detection setting of 60-s, and pluses indicate peaks using a setting of 30 s.

These findings thus do not support the hypothesis that rhythms become slower as cell number per group increases.

CLUSTER7 Analysis Supports Results Obtained with FFT

To further quantify the metabolic oscillations of beta cells and islets, CLUSTER7 was used to determine the interval, duration, and amplitude of peaks and nadirs within rh123 fluorescence patterns. Representative examples of fluorescence patterns from beta cells (Fig. 2A) and islets (Fig. 2B) demonstrated rhythms with periods ranging from approx 90 s (Fig. 2A, lower panel) to 7 min (Fig. 2B, lower panel). In some cases, changing the minimum parameters on CLUSTER7 revealed multiple rhythmic expressions as in Fig. 2A, lower panel, thus corroborating similar findings obtained using FFT.

The mean interval between peaks (e.g., the period of the oscillations) was typically shorter in dispersed beta cells using several different parameters in CLUSTER7, although this effect was statistically significant only when using the 120-s parameter for minimum period (Table 1). The lack of significance for the other parameters may be due, in part, to CLUSTER7's weakness in detecting peaks near the beginning or end of the data series, as evidenced by an undetected, but visually apparent, peak near the beginning of the series in Fig. 2A, upper panel. Patterns of activity in single beta cells also often appeared to be more irregular (less oscillatory) than patterns observed in intact islets (for example, see Fig. 2A, lower panel). While this could be a consequence of greater noise due to reduced signal averaging in single beta cells (which are much smaller than islets), it may also be indicative of metabolic differences. In general, both FFT and CLUSTER7 analysis support the finding that rhythms in dispersed beta cells are faster than in islets as summarized in Fig. 3A.

Amplitude of Oscillations

On average, the amplitude of beta-cell oscillatory peaks was greater than in islets (Table 1 and Fig. 3B). This result must be interpreted with caution, however. Because the ROI for islets is much larger than for dispersed beta cells, signal averaging greatly increases their signal to noise ratio (see Figs. 4A,C for an example of signals on the same scale). This noise reduction can also reduce the height of the detected peaks, thus possibly generating an artifactual difference between beta cells and islets. To attempt to adjust for these differences, point-to-point noise was determined for a sub-

Table 1
Summary of CLUSTER7 Findings

	Setting (s)	Interval (s)	Duration (s)	Amplitude (%)
	12	119 ± 13	91 ± 15	15.0 ± 1.4
Beta cells	30	132 ± 8	85 ± 10	12.5 ± 0.8
	60	156 ± 9	120 ± 11	12.2 ± 0.8
	120	169 ± 6	140 ± 15	10.6 ± 0.9
	12 (n = 2)	N/A[a]	N/A	N/A
Islets	30	163 ± 18	118 ± 25	7.5 ± 0.8*
	60	193 ± 37	164 ± 20	7.1 ± 0.3*
	120	320 ± 14*	205 ± 21*	7.7 ± 0.7*

[a]N/A, based on irregular intervals in only n of 2.
*$p < 0.025$.

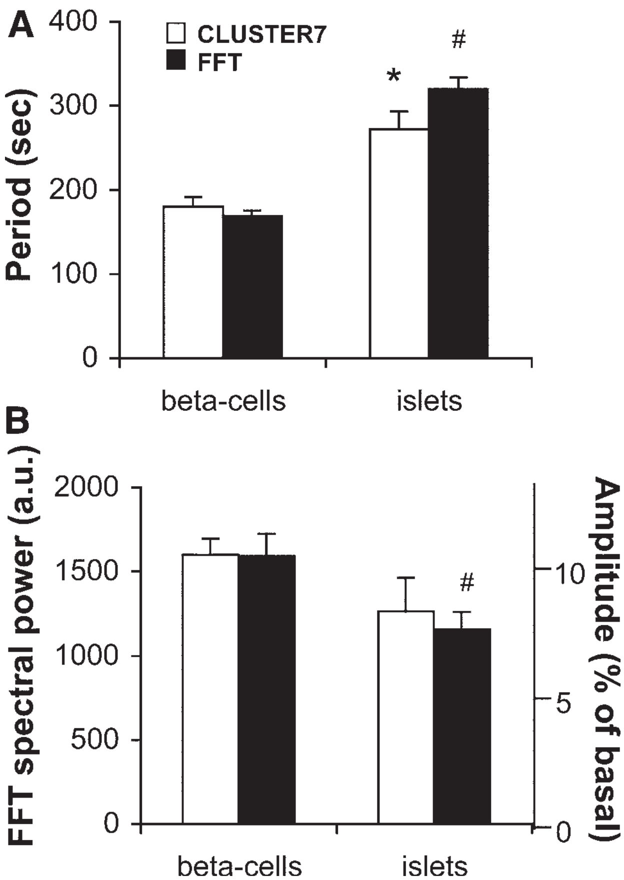

Fig. 3. Summary of findings. (**A**) Mean period of oscillations was determined for FFT (white bar) or CLUSTER7 (black bar) analysis for both beta cells and islets. (**B**) Mean "amplitude" of oscillations was determined as mean spectral power for FFT (white bar) and as percentage change from basal fluorescence for CLUSTER7 (black bar) for both beta cells and islets. Asterisks indicate a significant difference between groups by FFT ($p < 0.001$), and # represents significant differences for CLUSTER7 ($p < 0.02$).

set of recordings from beta cells (22.1 ± 1.8 a.u., $n = 16$) and islets (13.0 ± 2.7 a.u., $n = 16$). Noise from beta cells was reduced to 13.0 ± 0.9 a.u. using a two-point moving average, and the data were then reanalyzed. Although signal noise was reduced by over 40%, the oscillatory amplitude was reduced by approx 20%, and remained significantly larger than the amplitude of the corresponding signals in islets (beta cells: 11.1 ± 1.0%, islets: 7.1 ± 0.8%, $p < 0.005$). Signal noise was thus responsible for only part of the difference in the amplitudes of islet and beta cell oscillations, suggesting that other factors are responsible for these differences.

Mitochondria in Dispersed Beta Cells Are Less Energized Than in Islets

The larger amplitude oscillations that we observed in single beta cells suggest that single beta cells could actually have more energized mitochondria. We thus turned to a more direct pharmacological approach to determine how much energy is stored within $\Delta\Psi_m$. To determine the degree to which $\Delta\Psi_m$ is hyperpolarized (energized) under our experimental conditions, the mitochondrial poison NaN_3, which dissipates $\Delta\Psi_m$ to approx 0 mV, was applied after assessing baseline fluorescence for 28 islets and 44 beta cells. As shown in Fig. 4A, the fluorescence levels during NaN_3 treatment were approximately the same for the islet and beta cell shown in this representative example. This indicates, however, that the islet was significantly more hyperpolarized prior to this NaN_3 treatment (Fig. 4A). The mean response to NaN_3, displayed as percentage increase over control fluorescence levels, was also significantly greater in islets (Fig. 4B, $p < 0.02$). This suggests that islet mitochondria are more energized than dispersed beta-cell mitochondria.

We have reported previously that calcium levels are elevated in dispersed beta cells as compared to islets *(4)*. To test the hypothesis that elevated calcium levels account for the depolarized state of mitochondria in the dispersed beta cells, nifedipine was applied prior to NaN_3 in a subset of recordings to block calcium channels and reduce $[Ca^{2+}]_i$. As the example in Fig. 4C demonstrates, when fluorescence was normalized to NaN_3 treatment, $\Delta\Psi_m$ was clearly more depolarized during the control period, while the fluores-

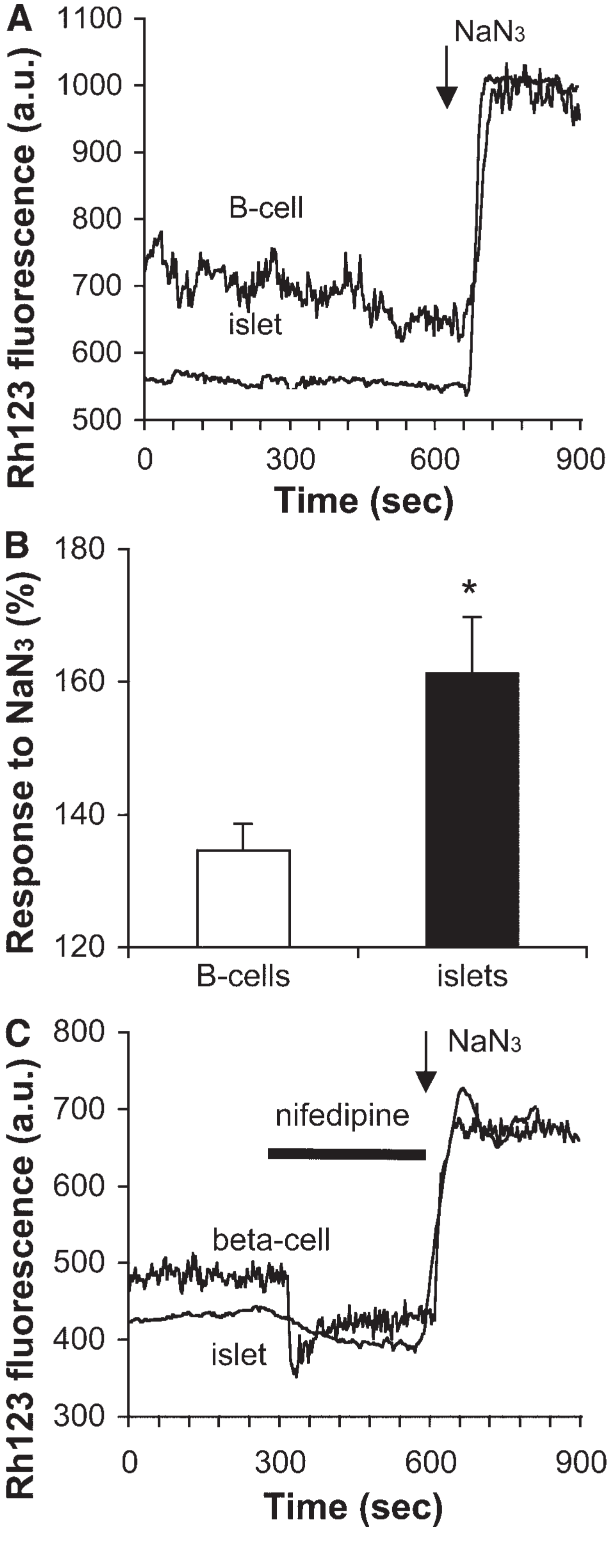

Fig. 4. Fluorescence change in response to NaN_3 suggests that calcium levels are elevated in dispersed beta cells. (**A**) Plot of rh123 fluorescence vs time for a representative beta cell and islet, normalized to a 5-min NaN_3 treatment following a 10-min baseline measurement. (**B**) Mean response to NaN_3 plotted as a fractional increase above baseline. (**C**) Plot of fluorescence vs time for a representative beta cell and islet, normalized to a 5-min NaN_3 treatment following a 10-min baseline measurement and 5-min treatment with the L-type calcium channel blocker nifedipine.

cence levels were similar when calcium influx was blocked by nifedipine. On average, nifedipine treatment hyperpolarized beta cells from control conditions by 15 ± 4% (n = 23) as compared to only 8 ± 1% for islets (n = 6), suggesting a greater effect of reducing calcium influx on $\Delta\Psi_m$ in dispersed beta cells. The resulting change in fluorescence from nifedipine to NaN_3 treatment resulted in a 61% increase, which approximates the response found in islets under control conditions (58 ± 9%). These findings suggest differences in $[Ca^{2+}]_i$ represent one possible mechanism mediating differences in mitochondrial activity between islets and dispersed beta cells.

Discussion

In this study, oscillations in $\Delta\Psi_m$ were observed in both cultured mouse islets and cultures of dispersed beta cells, suggesting that both preparations possess the necessary machinery to generate metabolic oscillations. These slow rhythms are consistent with the firing patterns, $[Ca^{2+}]_i$ oscillations, and metabolic oscillations observed previously in beta cells and islets by rh123 *(11–13)* and other techniques *(3,4,8,9)*. Differences in oscillatory period between beta cells and islets suggest that incorporation into islets may provide additional modulatory influences on a metabolic oscillator that is fundamental to the functioning of individual beta cells.

One source of modulatory influences could be provided by factors secreted by other cell types within islets, such as glucagon secreted by alpha cells, somatostatin secreted by delta cells, and pancreatic polypeptide secreted by PP cells. Alpha and delta cells, for example, have been shown to have their own intrinsic rhythmicity *(15,16)*. These cells types represent <20% of islet mass, with the vast majority composed of beta cells (see also Materials and Methods). We would expect that with beta cells being the dominant player, the influence of other cell types on islet rhythms may be limited, and thus only modulatory. Furthermore, the rhythms observed in alpha and delta cells recorded from intact islets occur independently of beta cell rhythms *(15)*, leading these authors to conclude that only beta cells are coupled to other beta cells. Factors secreted from non–beta cells could nevertheless act in a paracrine manner on beta cells.

Another difference between islet and beta cells was that islet mitochondria appeared to be more energized in comparison to the mitochondria from dispersed beta cells. The differences in mitochondrial energy storage may be due, in part, to the higher levels of $[Ca^{2+}]_i$ in dispersed beta cells, which, in turn, may depolarize $\Delta\Psi_m$ to a greater extent *(11, 13)*. Mitochondrial responses to nifedipine suggest that dispersed beta cells may have higher $[Ca^{2+}]_i$, as reported in a previous study comparing the $[Ca^{2+}]_i$ levels of islets and beta cells *(4)*. $\Delta\Psi_m$ and $[Ca^{2+}]_i$ are also often closely linked *(11–13)*, with peaks in $[Ca^{2+}]_i$ correlating to nadirs in mitochondrial energy (peaks in fluorescence indicating $\Delta\Psi_m$

is depolarized). Although these reports did not quantify these oscillations in mitochondrial activity and $[Ca^{2+}]_i$, the period appears to range between 1 and 5 min for both islets and beta cells *(11–13)*, which is consistent with our findings. While it is not presently known whether metabolic oscillations lead $[Ca^{2+}]_i$ oscillations or vice versa, the synchronicity of calcium and $\Delta\Psi_m$ suggests that mitochondrial activity and $[Ca^{2+}]_i$ are closely linked. The elevated calcium levels observed in dispersed beta cells could have an effect on communication between the mitochondria and the cell membrane. Beta-cell incorporation into islets thus may help the beta cells to maintain a larger mitochondrial gradient for increased ATP production, which would be consistent with the enhanced insulin secretion observed in islets.

Although this link between calcium and mitochondrial activity supports the findings of prior studies showing that secretion in islets is enhanced in comparison to dispersed beta cells, there are other possibilities. Chief among these is gap junction communication, which is prominent in islets but absent in isolated beta cells *(6,7)*. Gap junctions affect ion flux, and thus membrane potential, which is part of the secretory pathway. Transport of metabolites in and out of beta cells may also be affected, which could influence metabolic rhythms. The loss of coupling experienced by single beta cells may also increase local environmental influences. These influences can increase ion channel noise *(17)* and perturb normal rhythms, which may explain, in part, the increased irregularity of rhythms as we report.

In conclusion, our findings indicate that a slow metabolic oscillator is present in both single beta cells and islets. Our data thus suggest that shifts in $[Ca^{2+}]_i$ levels may be responsible for the differences between islets and dispersed beta cells in both metabolic rhythms and the pathways related to secretion. Although differences in mitochondrial activity thus appear to exist between islets and dispersed beta cells, additional studies will be required to determine if these differences contribute to variations in patterns of intracellular calcium, electrical activity, and insulin secretion.

Materials and Methods

Tissue Preparation

Mouse islets were isolated by collagenase from the pancreata of Swiss–Webster mice (age 2–3 mo, weight 25–35 g) as previously described *(18,19)*. All procedures were approved by the Animal Care and Use Committee of Virginia Commonwealth University, and all chemicals were purchased from Sigma-Aldrich (St. Louis, MO) unless otherwise stated. Islets were dispersed into single beta cells by gently pipetting islets in a low-calcium medium *(20)*. Islets or beta cells were deposited on glass coverslips pretreated with 0.1% gelatin (Gibco, Grand Island, NY) in 35-mm Petri dishes and cultured in RPMI-1640 medium supplemented with 10% fetal bovine serum, 1% L-glutamine, and 1% penicillin/streptomycin (Gibco). All cultures were incubated at 37°C in a 95/5% air/CO_2 mixture. Beta cells and islets were fed 1–2 d after preparation and were cultured for up to 4 d.

Fluorescence Measurements

Rh123 is an established fluorescent probe that has been used in numerous studies to determine $\Delta\Psi_m$ in living cells *(21,22)*, including beta cells *(10–13)*. We determined that rh123 more effectively penetrates the interior of islets compared to other mitochondrial dyes, such as TMRE. Procedures related to cell loading and fluorescence measurement have recently been described *(13)*. Briefly, beta-cell cultures or islets were loaded with 5 μ*M* rh123 for 10–15 min and incubated at 37°C, washed, and transported to a recording chamber. Rh123 fluorescence measurements were made on an Olympus BX61W1 upright laser-scanning confocal microscope using the FluoView acquisition system (excitation/emission of 488/535 nm; Olympus, Tokyo, Japan). Cells or islets were imaged every 3 s for 10–20 min.

To determine the mean fluorescence of images for analysis, rectangles were drawn around each islet, cell, or cluster, to form a region of interest (ROI). While we cannot exclude the possibility that some of our single cell recording were made from other cell types, such as alpha, delta, or PP cells, over 80% of islet cells cultured using our standard protocol are beta cells *(4,18)*. Furthermore, alpha cells do not tend to be oscillatory at high glucose concentrations *(15)*, so it is unlikely that alpha cells were oscillatory under our experimental conditions. Also, although we did not specifically select against them, very small cells (which were likely alpha cells based on size) did not typically display rhythms (in 11.1 m*M* glucose) and thus were not analyzed. While signals from delta cells and PP cells are more difficult to distinguish from beta cells, however, they represent a small fraction of total islet cells. Thus, a large majority of cells used in this study were very likely to be beta cells. For simplicity, all ROIs drawn around beta cells and clusters will be termed "beta cells" from hereon. Mean fluorescence among all pixels within each ROI was calculated for each image at 3-s intervals and plotted in arbitrary units of fluorescence (a.u.) vs time. These data series were then analyzed using FFT and CLUSTER7. Note that for presentation as figures, data series were graphed as a 10-point moving average to accentuate oscillations, and also in some cases baseline subtracted to level the trace.

Fast Fourier Transform Analysis

Data series were baseline-subtracted from the mean fluorescence, zero-padded at each end to at least two times the original data series length to eliminate circular correlation effects in derived Fourier power/frequency spectra *(23)*, and then smoothed with a Hanning function. Fast Fourier transform was performed using IGOR Pro version 4 (Wavemetrics, Lake Oswago, OR). For each data series, the frequency with the greatest spectral power was considered the dominant rhythmic frequency. Note that no spectral peak with a corresponding period larger than half the length of the data series was considered, because such observations could be associated with baseline drift rather than a repeated oscillatory pattern. Mean period was calculated as the inverse of the mean frequency. The corresponding fraction of spectral power in the specified period range relative to the total spectral power represented in the spectrum as a whole was also reported as an indicator of amplitude of oscillations.

CLUSTER7 Analysis

Additional analysis was performed on rh123 fluorescence patterns over the duration of each recording using the CLUSTER7 pulse detection algorithm *(24)*. CLUSTER7 compares clusters of data points by a pooled *t*-test to look for peaks and nadirs over time. Using a standard deviation of 5% of the baseline signal, CLUSTER7 identified oscillations in rh123 fluorescence in several data series. For each beta cell or islet, mean amplitude, duration, and interval of oscillations were calculated by averaging values from all peaks detected within the recording. Minimum oscillatory durations were set at 2, 5, 10, and 20 data points to identify each peak and nadir corresponding to a minimum oscillatory periodicity of 12, 30, 60, and 120 s, respectively. The minimum parameters exceeded the Nyquist frequency, which was 1/6 s in this case.

Additional Analysis

Responses to the mitochondrial poison NaN_3 or the L-type calcium channel blocker nifedipine were determined by comparing the mean fluorescence of images during the first 10 min of each recording (control phase) and the last 2 min of the drug treatment. Responses to NaN_3 or nifedipine were then expressed as the percent change from control values for each record. All comparisons between beta cells and islets were made using a two-tailed *t*-test assuming unequal variance (mean ± SEM).

Acknowledgments

Support provided by NIH grants DK-46409 to L.S.S. and F32 DK-065462 to C.S.N. We thank Sophia Gruszecki for assistance in tissue preparation, and Drs. Richard Bertram, Arthur Sherman, Min Zhang, and Paulette Goforth for editorial comments and helpful discussions.

References

1. Deeney, J. T., Prentki, M., and Corkey, B. E. (2000). *Semin. Cell Dev. Biol.* **11,** 267–275.
2. Henquin, J. C., Jonas, J. C., and Gilon, P. (1998). *Diabetes Metab.* **24,** 30–36.
3. Jonkers, F. C., Jonas, J. C., Gilon, P., and Henquin, J. C. (1999). *J. Physiol.* **520(Pt 3),** 839–849.
4. Zhang, M., Goforth, P., Bertram, R., Sherman, A., and Satin, L. (2003). *Biophys. J.* **84,** 2852–2870.
5. Gopel, S., Zhang, Q., Eliasson, L., et al. (2004). *J. Physiol.* **556,** 711–726.
6. Charollais, A., Gjinovci, A., Huarte, J., et al. (2000). *J. Clin. Invest.* **106,** 235–243.
7. Serre-Beinier, V., Mas, C., Calabrese, A., et al. (2002). *Biol. Cell* **94,** 477–492.
8. Jung, S. K., Kauri, L. M., Qian, W. J., and Kennedy, R. T. (2000). *J. Biol. Chem.* **275,** 6642–6650.
9. Porterfield, D. M., Corkey, R. F., Sanger, R. H., Tornheim, K., Smith, P. J., and Corkey, B. E. (2000). *Diabetes* **49,** 1511–1516.
10. Duchen, M. R., Smith, P. A., and Ashcroft, F. M. (1993). *Biochem. J.* **294(Pt 1),** 35–42.
11. Kindmark, H., Kohler, M., Brown, G., Branstrom, R., Larsson, O., and Berggren, P. O. (2001). *J. Biol. Chem.* **276,** 34530–34536.
12. Krippeit-Drews, P., Dufer, M., and Drews, G. (2000). *Biochem. Biophys. Res. Commun.* **267,** 179–183.
13. Nunemaker, C. S., Zhang, M., and Satin, L. S. (2004). *Diabetes* **53,** 1765–1772.
14. Jouaville, L. S., Pinton, P., Bastianutto, C., Rutter, G. A., and Rizzuto, R. (1999). *Proc. Natl. Acad. Sci. USA* **96,** 13807–13812.
15. Nadal, A., Quesada, I., and Soria, B. (1999). *J. Physiol.* **517 (Pt 1),** 85–93.
16. Berts, A., Gylfe, E., and Hellman, B. (1997). *Endocrine* **6,** 79–83.
17. De Vries, G. and Sherman, A. (2000). *J. Theor. Biol.* **207,** 513–530.
18. Hopkins, W. F., Satin, L. S., and Cook, D. L. (1991). *J. Membr. Biol.* **119,** 229–239.
19. Khan, F. A., Goforth, P. B., Zhang, M., and Satin, L. S. (2001). *Diabetes* **50,** 2192–2198.
20. Lernmark, A. (1974). *Diabetologia* **10,** 431–438.
21. Ronot, X., Benel, L., Adolphe, M., and Mounolou, J. C. (1986). *Biol. Cell* **57,** 1–7.
22. Chen, L. B. (1988). *Annu. Rev. Cell Biol.* **4,** 155–181.
23. Nunemaker, C. S., Straume, M., DeFazio, R. A., and Moenter, S. M. (2003). *Endocrinology* **144,** 823–831.
24. Veldhuis, J. D. and Johnson, M. L. (1986). *Am. J. Physiol.* **250,** E486–E493.